Study of Magnesium-Dopped Zinc Oxide Thin Films for Pb-Free PSCs Application

Muhamad Faiq Aiman Mat Yajid, Md. Jakir Hossen, Hairul Mardiah Hamzah, Noorhayati Idros, and Mohammad Aminul Islam*

Department of Electrical Engineering, Faculty of Engineering, Universiti Malaya
50603 Kuala Lumpur, Malaysia

E-mail: aminul.islam@um.edu.my

Abstract. Zinc oxide (ZnO) thin films are widely used in various types of solar cells; however, there are notable limitations, such as low electron mobility and surface defects, which affect the stability and efficiency of perovskite solar cells (PSCs). This study investigates the impact of magnesium (Mg) doping on the characteristics of ZnO thin films, prepared by spin coating, with the aim of enhancing PSC performance and stability. The films were characterized utilizing UV-Vis spectroscopy, field emission scanning electron microscopy (FESEM), energy-dispersive X-ray spectroscopy (EDX) and Hall Effect measurements. Additionally, the full device was simulated based on parameters obtained experimentally. We propose a novel Pb-free PSC and analyzed its performance utilizing both ZnO and ZnO:Mg thin films, as the electron transport layer. The results indicate that Mg doping enhances the electro-optical properties of ZnO, improving device efficiency to 21.83%. These advantageous effects of Mg doping mark a significant step toward achieving high-efficiency, durable photovoltaic devices, and advancing sustainable energy applications.

Keywords. ZnO; Mg Doping; Pb-free; PSCs; Bandgap; Solar Cells.

1. Introduction

Zinc Oxide (ZnO) thin films are semiconductor materials that have garnered significant interest due to their versatile applications in industries such as electronics, sensors, and notably, solar cell technology. These thin films are commonly produced using techniques like Atomic Layer Deposition (ALD), sputtering, Chemical Vapor Deposition (CVD), or spin coating onto substrates such as glass and silicon. ZnO thin films play a crucial role in the functionality of solar cells, serving as Transparent Conductive Oxides (TCOs) and/or window layers. When properly doped, ZnO thin films exhibit both transparency and electrical conductivity, making them ideal for use as transparent electrodes in solar cells. This allows incident light to pass through while enabling efficient charge carrier collection. Furthermore, the electronic properties of ZnO make it an excellent choice as an Electron Transport Layer (ETL) in certain types of solar cells, facilitating efficient electron extraction and transport.

ZnO offers several advantages over other materials used in solar cells. Its high electron mobility ensures efficient charge transport and minimizes electron recombination, ultimately enhancing solar cell performance. Additionally, the wide bandgap of ZnO limits sunlight absorption, allowing most of the incident light to pass through and reach the active semiconductor layer, thereby optimizing energy conversion efficiency [1].

Various techniques are employed to enhance the performance of ZnO thin films in solar cell applications. Controlled doping with elements such as aluminum, gallium, or magnesium can modify the properties of ZnO, improving its electrical conductivity and optical transparency. These modifications can increase the surface area, enhance light trapping, and influence charge carrier dynamics, all of which contribute to higher solar cell efficiency. Moreover, optimizing the interface between the ZnO layer and the active layer, as well as controlling the ZnO layer's thickness, significantly affects light transmission, electrical properties, and interface interactions, further improving solar cell performance [2].

Ongoing research into material synthesis, device engineering, and a deeper understanding of ZnO's fundamental properties is expected to drive further advancements, broadening its applications in solar energy conversion technologies. Research on magnesium doping in zinc oxide thin films for Perovskite solar cells (PSCs) is motivated by the need to boost both the efficiency and stability of PSCs. While PSCs exhibit tremendous potential as a sustainable energy solution due to their high efficiency, challenges such as long-term stability remain unresolved. ZnO thin films are commonly used as electron transport materials in PSCs, but there is growing need to explore innovative approaches to further improve their properties.

Magnesium doping presents a promising avenue to enhance the characteristics of ZnO thin films, potentially improving charge transport, light absorption, and device stability. Understanding how magnesium doping affects these thin films is crucial for overcoming current limitations and advancing the practical application of PSCs.

Research has shown that magnesium doping improves the structural, optical, and electrical properties of ZnO thin films, making them more effective as electron transport materials. Magnesium-doped ZnO enhances conductivity, light transmission, and reduces recombination losses, thus boosting PSC performance. Various synthesis methods have been explored to optimize doping for greater stability and efficiency in solar applications [3, 4].

This study seeks to investigate how magnesium doping influences ZnO thin films, aiming to identify improvements in material properties. The goal is to contribute to the development of highly efficient, stable, and commercially viable PSC technology, addressing key challenges in solar cell performance and accelerating the transition to a sustainable energy future.

2. Methods

2.1. Materials

Fluorine-doped Tin Oxide (FTO)/Soda lime glasses, ethanol, acetone, deionized water (18.2 MΩ), zinc acetate tetrahydrate, ethanolamine, magnesium nitrate.

2.2. Fabrication of ZnO:Mg

To deposit a thin film, commercially available soda lime glasses were cleaned in an ultrasonic bath degreased with ethanol-acetone-ethanol and deionized water for 5 min each. Degreased glasses were dried in the ambient using a hot plate at 80 ºC. To fabricate ZnO, 2.195 g zinc acetate tetrahydrate and 0.625 g ethanolamine were dissolved in 100 ml ethanol. The solution was stirred for approximately 30 min and filtered to achieve a uniform solution without residue. The glass substrates were placed on a spin coater and 3-4 drops of the solution were applied to the surface of the glass. The substrate was then spun at 1000 rpm for 10 seconds, followed by 4000 rpm for 40 seconds, and finally at 1000 rpm for 10 seconds. The films were annealed at 300°C for 20 minutes. Magnesium-doped ZnO films were fabricated by adding magnesium nitrate at 1% concentrations to the ZnO solution, which was then stirred for uniform distribution, followed by the same spin-coating and annealing process.

2.3. Characterization Techniques

Surface morphology, including grain size and grain growth, was observed using Scanning Electron Microscope (SEM) images taken with the “LEO 1450 Vp’ instrument, which also conducted elemental analysis using Energy-Dispersive X-ray Spectroscopy (EDX). Optical properties, such as transmittance and bandgap, were measured with UV-vis spectrometry using the ‘Perkin Elmer Instruments Lambda35’. Carrier concentration, mobility, and resistivity were analyzed using the Hall measurement system ‘ECOPIA 3000’Fluorine-doped Tin Oxide (FTO)/Soda lime glasses, ethanol, acetone, deionized water (18.2 MΩ), zinc acetate tetrahydrate, ethanolamine, magnesium nitrate.

2.4. Device Simulation

In this study, the widely used solar cell simulation software 'SCAPS-1D' was employed to evaluate the effect of magnesium-doped ZnO on the performance of planar PSCs. The simulation aimed to enhance understanding of the physical processes involved and to improve device efficiency. The impact of Mg doping was observed in PSC properties, indicating potential advantages for fabricating high-efficiency, highly stable PSCs. The parameters utilized in the device simulation are summarized in Table 1.

Table 1. Parameters in SCAPS-1D.

Parameter	**units**	**CuO**	**$Cs_2AgBiSbBr_6$**	**ZnO:Mg**	**FTO**
Thickness, w	nm	80	300	60 nm	200
Band Gap, Eg	eV	1.96	1.50	**From this study**	3.20
Electron affinity, Xe	eV	2.75	3.90	3.95	4.40
Permittivity, εr		12.48	10.00	10.00	9.00
CB effective density of states	cm^{-3}	2.20E+18	2.20E+18	4.00E+18	5.200E+18
VB effective density of states	cm^{-3}	1.8E+19	1.8E+19	9.00E+18	1.000E+18
Electron mobility, µn	cm^2/Vs	3.99E+0	1.00E+1	**From this study**	1.000E+1
Hole mobility, µp	cm^2/Vs	3.99E+0	1.00E+1	0	1.000E+1
Electrothermalvelocity	cm/s	1.00E+7	1.00E+7	1.00E+7	1.00E+7
Hole thermalvelocity	cm/s	1.00E+7	1.00E+7	1.00E+7	1.00E+7
Shallow uniform donor density, ND	cm^{-3}	0	2.00E+16	2.00E+16	1.00E+20
Shallow uniform acceptor density NA	cm^{-3}	2.44E+16	2.00E+10	0	0
References		[5]	[6]	[7]	[8]

3. Results and Discussion

Significant changes in the surface morphology of the fabricated ZnO and ZnO:Mg films are observed in Fig. 1 (a) and Fig. 1 (b). The undoped ZnO displays a granular surface with loosely packed particles, contributing to non-uniformity and potential variations in its optical and electrical properties. In contrast, magnesium-doped ZnO exhibits a more uniform and evenly distributed particle arrangement. This enhanced homogeneity and smooth surface morphology, resulting from Mg doping improves the optical transparency and electrical conductivity of the ZnO film, making it highly suitable for applications like transparent conductive electrodes and thin-film transistors.

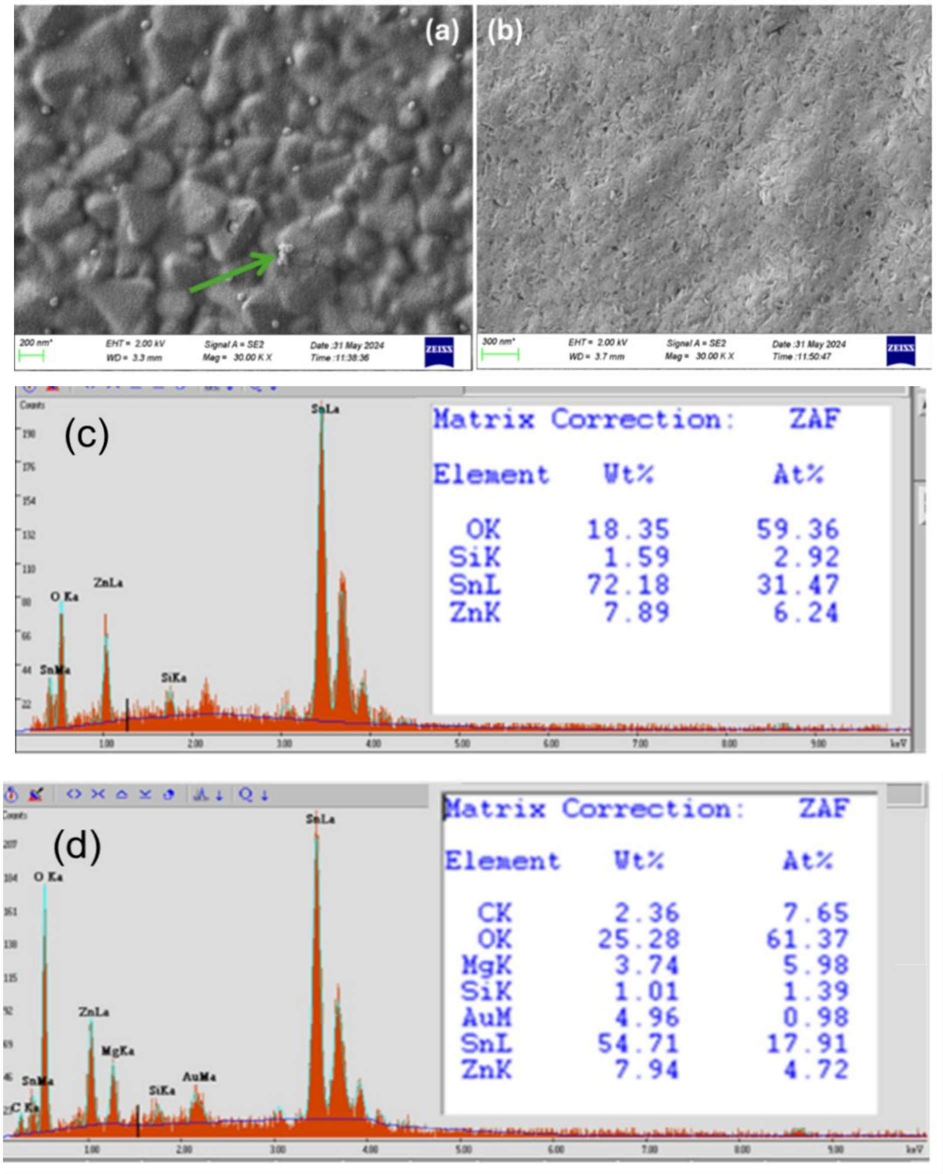

Matrix Correction: ZAF

Element	Wt%	At%
OK	18.35	59.36
SiK	1.59	2.92
SnL	72.18	31.47
ZnK	7.89	6.24

Matrix Correction: ZAF

Element	Wt%	At%
CK	2.36	7.65
OK	25.28	61.37
MgK	3.74	5.98
SiK	1.01	1.39
AuM	4.96	0.98
SnL	54.71	17.91
ZnK	7.94	4.72

Figure 1. Surface morphology of thin films, their elemental composition and EDX spectrum of undoped ZnO (a, c), and ZnO: Mg (b, d).

Figures 1(c) and 1(d) present the elemental analysis of the films. The analysis displays high concentrations of zinc (Zn) and oxygen (O), with O at 18.35% wt% and 59.36% at%, and Zn at 7.89% wt% and 6.24% at%. Peaks for tin (Sn) and silicon (Si) are also observed, with Sn at 72.18% wt% and 31.47% at%, attributed to the Fluorine-doped Tin Oxide (FTO) glass substrate. The low Si presence likely results from trace contaminants. Figure 1 (b) further confirms successful Mg doping within the ZnO matrix, with Mg at 3.74% wt% and 5.98% at%. The oxygen and zinc levels are consistent with pure ZnO, showing O at 25.28% wt% and 61.37% at%, and Zn at 7.94% wt% and 4.72% at%.

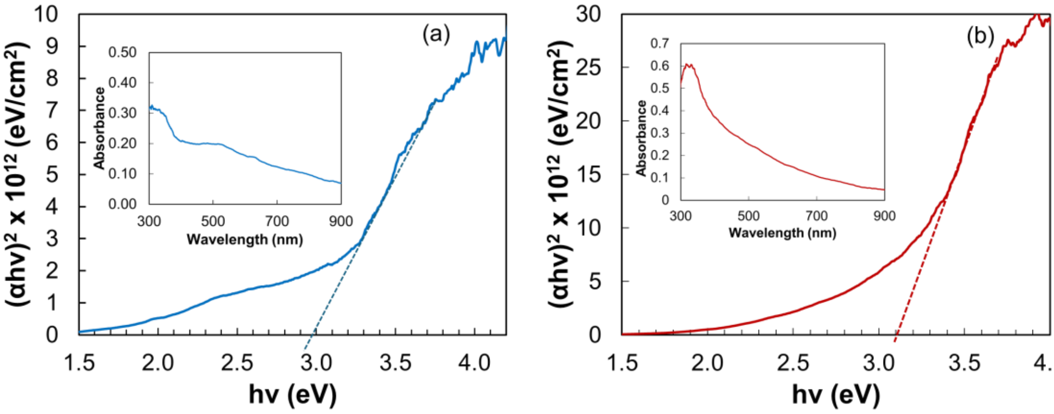

Figure 2. The photon energy of the (a) undoped ZnO and (b) ZnO:Mg thin films.

Figure 2 illustrates the optical properties of the prepared films, with the inset showing their absorbance spectra. As an electron transport layer, low absorbance is preferable to maximize light transmission to the active layer, enhancing photon absorption and photogenerated current. Proper elemental doping and post-deposition treatments improve crystallinity, reduce defects, and increase layer density, lowering absorbance.

The Tauc plot in Fig. 2(a), (b) was used to estimate the optical bandgap (Eg) by extrapolating the linear region at α=0, with values tabulated in Table 2. As-deposited ZnO bandgap increases from 2.98 eV to 3.10 eV upon Mg doping due to impurity effects and grain size differences, impacting optical transmittance and bandgap energy. The increase in optical band gap may result from metal impurities occupying sites outside the host lattice during film preparation and thermal treatment. These impurities can act as donor atoms, shifting the energy levels and making the band structure non-degenerate, thereby raising the bandgap energy [9].

Additionally, thin-film grain size greatly affects optical transmittance, which in turn affects optical bandgap. In particular, the bandgap and optical transmittance decrease with increasing grain size [10]. The FESEM images reveal those variations in grain size and surface roughness correlate with changes in the optical properties of the films. The ZnO film, which exhibited larger grains and a rougher surface compared to ZnO:Mg, showed a lower optical bandgap. This difference suggests that increased grain size and surface roughness in the ZnO film contribute to its reduced bandgap, as these structural factors impact optical transmittance and band structure.

Table 2. Bandgap and Hall Effect parameters of ZnO and ZnO: Mg thin film

Time (minutes)	**Bandgap (eV)**	**Carrier Concentration (cm^3/Vs)**	**Carrier Mobility (cm^2/Vs)**	**Resistivity**
ZnO	2.98	1.308E+17	1.013E+01	8.944E+02
ZnO:Mg	3.10	8.671E+17	2.354E+03	1.730E+02

Table 2 presents the electrical properties of the films as determined by Hall Effect measurements, showing that the ZnO:Mg film has a higher carrier concentration than undoped ZnO. This increase in carriers is likely due to Mg impurities acting as donors, which shift energy levels and reduce film resistivity. Additionally, ZnO:Mg films exhibited higher carrier mobility, as optimal Mg doping can improve mobility by reducing grain boundary scattering and defects. However, excessive doping might introduce scattering centers that impact mobility. Overall, Mg doping enhances ZnO's electrical properties, positively influencing PSC performance.

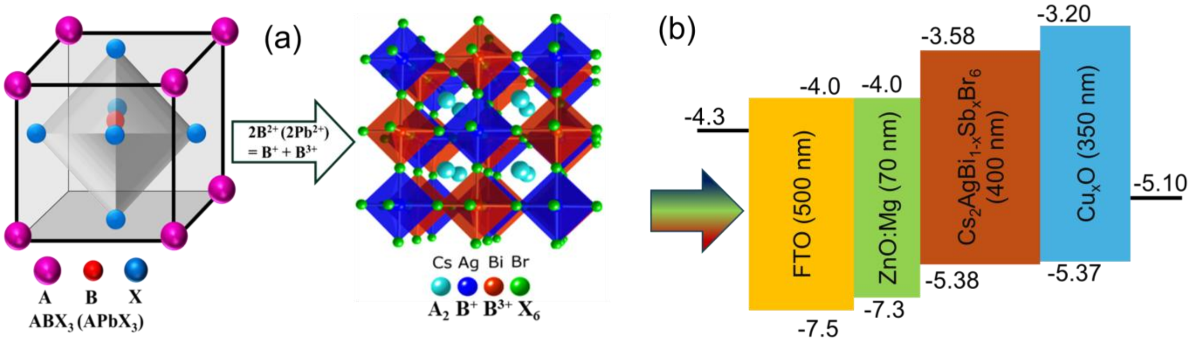

Figure 3. Schematic diagram of (a) replacement of $B+/B_3+$ cations in Pb halide perovskite ($APbX_3$) with double perovskite ($A_2B+B_3+X_6$) and (b) schematic band diagram of the proposed PSCs. Reproduced with permission [11].

The one-dimensional simulation program SCAPS-1D (version 3.3.01) was used to evaluate the performance of PSCs with ZnO and ZnO:Mg as electron transport layers (ETL). The proposed PSC has the configuration of FTO/ZnO: Mg/$Cs_2AgBi_{1-x}Sb_xBr_6$/Cu_xO/Au adopting a novel Cs-based halide double perovskite structure. A schematic band diagram of the proposed perovskite solar cell is depicted in Fig. 3(b). Optoelectronic properties of ZnO and ZnO: Mg were incorporated, with a thickness of 80nm for the ETL. Although $MAPbI_3$-based PSCs have achieved PCEs above 25%, concerns over Pb toxicity and instability have driven the search for non-toxic, stable alternatives. Materials such as tin, Germanium, Antimony, and Bismuth, along with their combinations, are being explored for photovoltaic applications. Among these, the $A_2B^+B^{3+}X_6$ structure (Figure 1 (a)), known as double perovskite, is the most stable. A-site materials (cations) are found within the cavities created by the octahedral in the double PVSKs, which have a 3D structure of Pb PVSKs with alternating $[B_3+X_6]^{3-}$ and $[B+X_6]^{5-}$ octahedral arranged in a 3D framework known as rock salt order. $Cs_2AgBi_{1-x}Sb_xBr_6$ lead-free double perovskite shows promise but still faces efficiency challenges [12]. Research is ongoing to improve its performance, with the photovoltaic community working to develop efficient PSCs using this material. Device performance results from simulations are shown in Fig. 4.

Figure 4(a) depicts the current-voltage (I-V) curves for devices with ZnO and ZnO:Mg as ETLs, with the inset table detailing the I-V characteristics. The device with ZnO:Mg demonstrates higher Power Conversion Efficiency (PCE), Filler Factor (FF), and current density, attributed to Mg doping, which improves ZnO's electrical properties by reducing defect density and increasing carrier concentration and mobility. Figure 4(b) shows C-V characteristics, indicating identical built-in potentials for both devices. Figure 4(c) illustrates the temperature effect on performance, showing a 0.1%/K temperature gradient, confirming Mg's positive impact. Additionally, the light intensity gradient of PCE is 0.45%, further supporting Mg doping’s benefit.

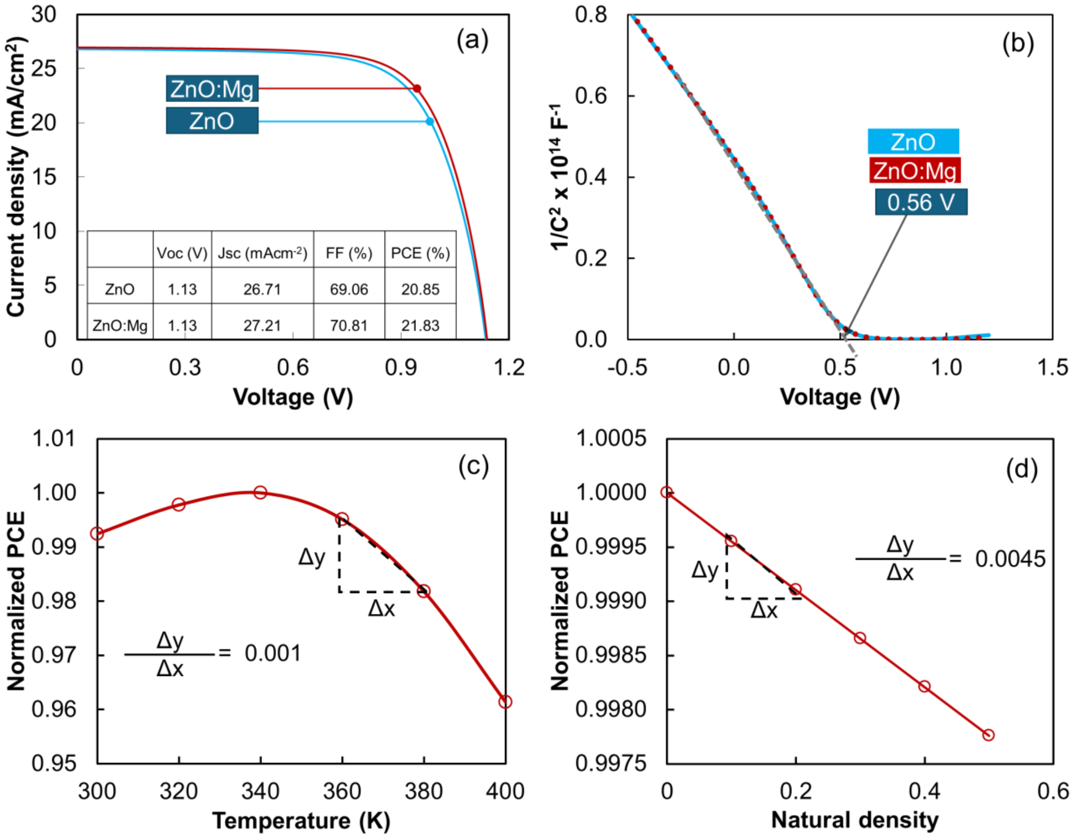

	Voc (V)	Jsc (mAcm^{-2})	FF (%)	PCE (%)
ZnO	1.13	26.71	69.06	20.85
ZnO:Mg	1.13	27.21	70.81	21.83

Figure 4. Comparison of (a) I-V curve, (b) C-V curve, (c) impact of temperature on the device performance, and (d) impact of light intensity on the device performance.

4. Conclusion

In this study, ZnO and Mg-doped ZnO thin films were successfully fabricated using a novel spin coating technique. It was found that ZnO:Mg exhibited superior electro-optical properties compared to the pure ZnO thin film. Specifically, Mg doping improved the electrical properties of ZnO by reducing defect density and increasing carrier concentration and mobility, which enhanced charge transfer and carrier collection. Additionally, the increased optical bandgap of ZnO:Mg improved light absorption and optimized the utilization of incident sunlight, contributing to a higher overall efficiency of the PSC. As a result, better device performance with a higher performance conversion efficiency (PCE) was observed when ZnO:Mg was used as the electron transport layer (ETL). The device with ZnO:Mg as the ETL and $Cs_2AgBi_{1-x}Sb_xBr_6$ as the absorber layer achieved an efficiency of 21.83%. This study demonstrates that doping the zinc oxide layer with magnesium significantly improves PSC efficiency, as confirmed by both experimental and simulation results. Future work will focus on optimizing the magnesium doping concentration in ZnO films to enhance electro-optical properties and device performance. Long-term stability testing will be conducted to assess durability under various environmental conditions. Additionally, alternative doping elements will be explored, and efforts will be made to scale up the fabrication process for large-area PSCs while maintaining performance. Interface optimization between the ZnO:Mg ETL and absorber layers, along with the investigation of advanced absorber materials, will be key to improving charge extraction and efficiency. Enhanced simulations will help refine device models, ultimately leading to more efficient, stable, and scalable ZnO:Mg-based PSCs for real-world applications.

Acknowledgements

The authors would like to thank the Faculty of Engineering, Universiti Malaya, for supporting this work.

References

[1] T. Ivanova, A. Harizanova, T. Koutzarova, B. Vertruyen, & R. Closset, Deposition of Sol–Gel ZnO:Mg Films and Investigation of Their Structural and Optical Properties, *Materials*, 15(2022)24. doi.org/10.3390/ma15248883.

[2] K. Salim, M. Medles, A. Nakrela, R. Miloua, A. Bouzidi, & R. Desfeux, Enhancement of optical and electrical properties of spray pyrolysed ZnO thin films obtained from nitrate chemical by Al-Sn co-doping. *Optik,* (2020) 210. doi.org/10.1016/j.ijleo.2020.164504.

[3] M. Manabeng, B. S. Mwankemwa, R. O. Ocaya, T. E. Motaung, & T. D. Malevu, Review of the Impact of Zinc Oxide Nanostructure Morphology on Perovskite Solar Cell Performance. *Processes*, 10 (2022) (9), 1803. doi.org/10.3390/pr10091803.

[4] X. Zhenga, T. Zhang, Metal Oxide Electron Transport Materials for Perovskite Solar Cells: A Review. *SpringerLink* (2020).

[5] Y. Ait-Wahmane, H. Mouhib, B. Ydir, A. Ait Hssi, L. Atourki, A. Ihlal, & K. Bouabid, Comparison study between ZnO and TiO_2 in CuO based solar cell using SCAPS-1D, *Materials Today: Proceedings* 52(2021), 166–171. doi.org/10.1016/j.matpr.2021.11.535.

[6] S. Kumar, A. Kumar, & V. Krishnan, Nanoscale zinc oxide-based heterojunctions as visible light active photocatalysts for hydrogen energy and environmental remediation, *Catalysis Reviews*, 62 (2019), 1–60. doi.org/10.1080/01614940.2019.1684649.

[7] E. Ghahremanirad, S. Olyaee, A. B. Nejand, P. Nazari, V. Ahmadi, & K. Abedi, Improving the performance of PSCs using kesterite meso-structure and plasmonic network, *Solar Energy*, 169(2018), 498–504. doi.org/10.1016/j.solener.2018.05.012.

[8] I. Alam, & A. Ashraf, Effect of Different Device Parameters on Tin Based Perovskite Solar Cell Coupled with In_2S_3 Electron Transport Layer and CuSCN and Spiro-OMeTAD Alternative Hole Transport Layers for High Efficiency Performance, (2020).

[9] M. Shahinuzzaman, M. A. Islam, S. Afroz, M. Hossain, M. S. Jamal, A. M. Alanazi, & M. Akhtaruzzaman, Synthesis of tungsten-doped zinc oxide nanoparticles using Aloe vera extracts for PSCs. *Optik,* 313(2024), 172006.

[10] T.M. Demiriz &A. Peksoz, The sensitive control of semiconductor properties of non-vacuum and electrochemically synthesized CdTe thin films, *Journal of Materials Science: Materials in Electronics*, 30 (2019) (9):8645-54. doi.org/10.1007/s10854-019-01187-2.

[11] M. J. Hossen, M. B. Rahman, M.H. Miah, Modeling and optimization of high efficiency Pb-free Cs-based-halide double perovskite solar cell using SCAPS-1D, *J Opt* (2025). doi.org/10.1007/s12596-025-02550-9.

[12] M. J. Hossen, H. M. Hamzah, M. Shahinuzzaman, M.S. Jamal, S. M. Said, S. F. W. M. Hatta, M. H. Miah, M. U. Khandaker and M. A. Islam, Recent progress on the efficiency and stability of lead-free $Cs_2AgBiBr_6$ double halide perovskite solar cells, *Physica Scripta* 100(2024), 012005. doi: 10.1088/1402-4896/ad9b59.